Channel Modeling for Heterogeneous Vehicular ISAC System with Shared Clusters

Baiping Xiong*†, Zaichen Zhang*†, Yingmeng Ge*†,
Haibo Wang*†, Hao Jiang*‡, Liang Wu*†, and Ziyang Zhang*†
*National Mobile Communications Research Laboratory, Southeast University, Nanjing 210096, China
†Purple Mountain Laboratories, Nanjing 211111, China
‡College of Artificial Intelligence, Nanjing University of Information Science and Technology, Nanjing 210044, China
Corresponding Author: Zaichen Zhang
Emails: {xiongbp, zczhang, ymge, haibowang}@seu.edu.cn, jianghao@nuist.edu.cn, {wuliang, ziyangzhang}@seu.edu.cn.

Abstract—In this paper, we consider the channel modeling of a heterogeneous vehicular integrated sensing and communication (ISAC) system, where a dual-functional multi-antenna base station (BS) intends to communicate with a multi-antenna vehicular receiver (MR) and sense the surrounding environments simultaneously. The time-varying complex channel impulse responses (CIRs) of the sensing and communication channels are derived, respectively, in which the sensing and communication channels are correlated with shared clusters. The proposed models show great generality for the capability in covering both monostatic and bistatic sensing scenarios, and as well for considering both static clusters/targets and mobile clusters/targets. Important channel statistical characteristics, including time-varying spatial cross-correlation function (CCF) and temporal auto-correlation function (ACF), are derived and analyzed. Numerically results are provided to show the propagation characteristics of the proposed ISAC channel model. Finally, the proposed model is validated via the agreement between theoretical and simulated as well as measurement results.

Index Terms—Channel model, integrated sensing and communications, heterogeneous vehicular system, shared clusters.

I. INTRODUCTION

With the ongoing commercial deployment of fifth generation (5G) wireless network all over the world, the field results have shown the shortcomings of 5G in meeting with the increasing requirements of the future, and therefore researchers are devoting their attention to the next generation wireless network [1]. Different from the previous generations of the wireless networks with one exclusive purpose of wireless communications, the future sixth generation (6G) wireless network is a heterogeneous network with an integration of various functions such as communications, sensing, computing, and controlling [2]. Specifically, the heterogeneous vehicular system provides low-latency high-throughput sensing and cooperation services, naturally inspiring the research on the integrated sensing and communications (ISAC) technology for contributing better performance from both academia and industry [3].

The ISAC is a design methodology including associate enabling technologies that integrates wireless sensing and communication capabilities into one system to realize efficient utilization of hardware as well as radio resources, and to achieve mutual benefits [2]. Specifically, the exploration of

higher frequency bands as well as the ubiquitous devices enables the wireless system to better understand the surrounding environments through radio propagation. The precise sensing results of the targets as well as the physical environments, on the other hand, can contribute to efficient communication algorithms design. In [4], the authors considered the dynamic frame structure design of a multi-vehicle ISAC system for the purpose of achieving low-latency and high-throughput sensing data sharing among vehicles, where results from the testbed validate the feasibility of the proposed design. The authors in [5] investigated the beamforming design of a ISAC vehicular system, where the results show that the communication beam tracking overheads could be significantly reduced with the assistance of sensing capability of ISAC.

For the development of ISAC, one of the indispensable aspects lies in the investigation of underlying propagation characteristics and development of appropriate channel models [6]. Thus far, only a few studies have involved in the ISAC channel research. The authors in [7] introduced the deterministic channel modeling approaches, including integral equation, physical optics, and geometrical optics, for sub-terahertz (THz) imaging scenarios, where the results show that the geometrical optics based modeling solution is more compatible with the measurements especially in three-dimensional (3D) imaging applications. In [8], the authors developed a 3GPP-extended channel model for ISAC scenario, where both communication and sensing channels are generated based on the 3GPP structure with random parameters. The authors in [9] proposed a 3D non-stationary ISAC channel model for monostatic sensing scenario, where a forward and backward scattering structure is considered for the communication channel. It is worth mentioning that the communication and sensing channels share the same time/space/frequency resources, indicating the existence of shared clusters/targets in ISAC channel. Different from communication channels with stochastically distributed clusters, the performance analysis of sensing channels heavily related to the deterministic locations of transceivers and clusters [7]. Also, the status of clusters/targets in ISAC channel show different impacts on the propagation properties. These, however, have not been involved in existing studies.

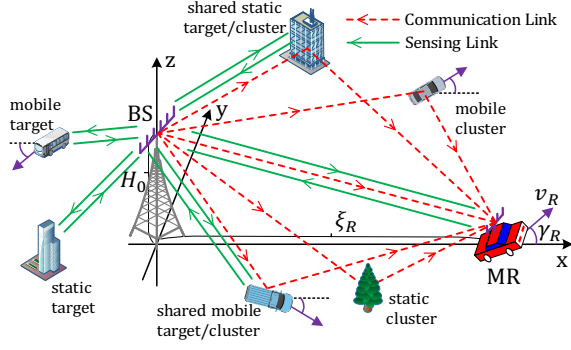To address the aforementioned issues, this paper develops

Fig. 1. A physical illustration of the proposed heterogeneous vehicular ISAC system with shared targets/clusters, taking monostatic sensing as an example.

$\xi_{\mathrm{MR}}^{T}(t), \xi_{\mathrm{MR}}^{R^e}(t)$	distances between BS/echo receiver and MR
$\xi_{s_{\ell_1}}^{T}, \xi_{s_{\ell_1}}^{R^e}$	distances between BS/echo receiver and s_{ℓ_1}
$\xi_{s_{\ell_2}}^{T}(t), \xi_{s_{\ell_2}}^{R^e}(t)$	distances between BS/echo receiver and s_{ℓ_2}
$\alpha_{T}^{i_2}(t), \beta_{T}^{i_2}(t)$	AAoD/EAoD from BS to target $i_2 \in \{\mathrm{MR}, s_{\ell_1}, s_{\ell_2}\}$
$\alpha_{R^e}^{i_2}(t), \beta_{R^e}^{i_2}(t)$	AAoA/EAoA from target $i_2 \in \{\mathrm{MR}, s_{\ell_1}, s_{\ell_2}\}$ to BS
$\xi_{s_{\ell_3}}^{T}, \xi_{s_{\ell_3}}^{R}(t)$	distances between BS/MR and s_{ℓ_3}
$\xi_{\ell_3, i_3}^{T}, \xi_{\ell_3, i_3}^{R}(t)$	distances between BS/MR and s_{ℓ_3} via i_3-th ray
$\xi_{s_{\ell_4}}^{T}(t), \xi_{s_{\ell_4}}^{R}(t)$	distances between BS/MR and s_{ℓ_4}
$\xi_{\ell_4, i_4}^{T}(t), \xi_{\ell_4, i_4}^{R}(t)$	distances between BS/MR and s_{ℓ_4} via i_4-th ray
$\alpha_{T}^{\ell_3, i_3}, \beta_{T}^{\ell_3, i_3}$	AAoD/EAoD from BS to s_{ℓ_3} via i_3-th ray
$\alpha_{R}^{\ell_3, i_3}(t), \beta_{R}^{\ell_3, i_3}(t)$	AAoA/EAoA from s_{ℓ_3} to MR via i_3-th ray
$\alpha_{T}^{\ell_4, i_4}(t), \beta_{T}^{\ell_4, i_4}(t)$	AAoD/EAoD from BS to s_{ℓ_4} via i_4-th ray
$\alpha_{R}^{\ell_4, i_4}(t), \beta_{R}^{\ell_4, i_4}(t)$	AAoA/EAoA from s_{ℓ_4} to MR via i_4-th ray

a general 3D non-stationary multi-antenna heterogeneous vehicular ISAC channel model applicable for both monostatic and bistatic sensing scenarios, where the channel responses of communication and sensing channels are separately derived. To characterize the unique properties of the heterogeneous vehicular ISAC system, we adopt the geometrical optics based deterministic model for characterizing sensing channel and the geometrical based stochastic model for characterizing the communication channel, respectively. The communication and sensing channels are partially correlated by considering a shared cluster structure, where both static clusters/targets and mobile clusters/targets are considered. The agreement between theoretical and simulated results as well as measurements validate the proposed model.

Notation: In this paper, non-boldface, boldface lowercase, and boldface uppercase letters denote scalar, vector, and matrix, respectively; $|\cdot|$, $(\cdot)^*$, and $\langle \cdot, \cdot \rangle$ stand for absolute value, complex conjugate, and vector dot product, respectively; $\mathbb{E}\{\cdot\}$ and $\cap$ take the expectation and intersection set, respectively.

II. SYSTEM MODEL

As illustrated in Fig. 1, we consider a heterogeneous vehicular ISAC system consisting of a static dual-functional base station (BS) with height H_0 and a ground mobile receiver (MR) with velocity vector $\mathbf{v}_R = v_R[\cos \gamma_R, \sin \gamma_R, 0]^T$, where v_R is the moving speed and γ_R is the moving direction, respectively. The dual-functional BS intends to communicate with the MR and at the same time sensing the surrounding environment. Different from the conventional communication system [10] and/or radar sensing system [11], where the signals are emitted by the BS with only one purpose in mind, either communicating with the receiver or sensing the target. In ISAC system, the signals transmitted by the BS are reused, taking the responsibilities for not only carrying the information bits to the receiver but also sensing the surrounding environment simultaneously. Therefore, the ISAC channel is consists of two parts, they are, the communication channel between the dual-functional BS and the communication receiver as well as the sensing channel between the dual-functional BS and the sensing targets, respectively. In this paper, the definition of the global coordinate system and that of the angular parameters

in the coordinate system follow the procedure in [12], where the projection of the center of BS transmit antenna array is defined as the origin and the line connecting the origin and the center of communication receiver's antenna array is defined as the x-axis, respectively. For ease of clarification, all antenna arrays are assumed to be uniform linear arrays (ULAs) with omnidirectional radiating pattern. The definitions of the key model parameters, including parameters for sensing and communication channels, are summarized in Table I.

In ISAC system, the dual-functional BS emits the dual-functional signals for communication and sensing purpose. Some of the transmitted dual-functional signals will travel through the communication channel to the communication receiver, others will impinge on the sensing targets, getting reflected by the targets, and then travel to the sensing receiver via the sensing channel. Based on the physical location of the sensing antenna array, the sensing sub-system in ISAC system is generally categorized as monostatic sensing, also known as active sensing, and bistatic sensing, also known as passive sensing, respectively [13]. In monostatic sensing, the antenna array is reused for both transmitting sensing signals and receiving the echo sensing signals, which is enabled by the development of full duplex antenna technology. In bistatic sensing, on the other hand, the sensing signal transmitting antenna array and the echo receiving antenna array are two different antenna arrays with physically separated locations, mounted either on the same platform or different platforms. To provide a general description, we assume the center of the sensing signal transmitting antenna array is mounted at position $(0, 0, H_0)$ with antenna number denoted by M_T and antenna element spacing denoted by δ_T, respectively. The orientation angle of the sensing signal transmitting ULA is defined as ψ_T in the azimuth direction and ϕ_T in the elevation direction, respectively. At the echo receiving side, the sensing signal receiving ULA is located at point $(x_{R^e}, y_{R^e}, z_{R^e})$ with antenna number and antenna element spacing denoted by M_{R^e} and δ_{R^e}, respectively. Similarly, we use ψ_{R^e} and ψ_{R^e} to represent the azimuth and elevation orientation angles of the echo receiving ULA, respectively. It can be seen that the proposed model can be adapted to characterize the monostatic sensing

Target Type	RCS [m²]
Automobile	100
Pickup truck	200
Adult	1
Bird	0.01
Insect	10^{-5}
Missile	0.5
Jumbo jet airliner	100
Large bomber	40
Small fighter aircraft	2

ISAC system when $x_{R^e} = 0$, $y_{R^e} = 0$, $z_{R^e} = H_0$, $M_{R^e} = M_T$, $\delta_{R^e} = \delta_T$, $\psi_{R^e} = \psi_T$, and $\phi_{R^e} = \phi_T$, respectively; otherwise, it characterizes a bistatic sensing ISAC system.

For the communication sub-system in the ISAC system, it shares the same transmitting ULA as the sensing sub-system, and therefore we use the same symbol notations for the transmit antenna parameters definition. As the communication receiver of the communication sub-system is concerned, the communication and sensing signal receiving ULAs are obviously not the same antenna array. In particular, the communication signal receiving ULA has M_R antennas, with antenna element spacing denoted by δ_R as well as antenna orientation angles denoted by ψ_R and ϕ_R in the azimuth and elevation directions, respectively. Moreover, the location of the center of the communication signal receiving ULA is at point $(\xi_R, 0, 0)$ at the initial instant, which yields to be $(\xi_R + v_R t \cos \gamma_R, v_R t \sin \gamma_R, 0)$ at time instant t.

A. Sensing Channel Modeling

In the sensing channel, the sensing targets span a wide range from the surrounding buildings, trees, and running vehicles, to the mobile communication receiver. In this case, we divide the targets into three categories, they are, the terminal target (e.g., communication receiver MR), the static targets (e.g., static buildings and trees, etc.), and the mobile targets (e.g., running vehicles and pedestrians, etc.), respectively. The NLoS propagations are ignored in sensing channel due to the high loss and reflection property of targets. We assume there are L_1 static targets forming a target set of C_{L_1} with the ℓ_1-th ($\ell_1 = 1, 2, ..., L_1$) target being denoted by s_{ℓ_1}, and assume there are L_2 mobile targets on the ground surface forming a target set of C_{L_2}. For the ℓ_2-th ($\ell_2 = 1, 2, ..., L_2$) mobile target in target set C_{L_2}, that is, s_{ℓ_2}, its velocity vector is represented by $\mathbf{v}_{\ell_2} = v_{\ell_2}[\cos \gamma_{\ell_2}, \sin \gamma_{\ell_2}, 0]^T$, in which v_{ℓ_2} and γ_{ℓ_2} denote the moving speed and direction of the target s_{ℓ_2}, respectively. Let $\mathbf{s}(t) \in \mathbb{C}^{M_T \times 1}$ denote the dual-functional transmitted signal vector and $\mathbf{y}^e(t) \in \mathbb{C}^{M_{R^e} \times 1}$ denote the received echo signal vector, respectively. Then, the received signal model for the sensing sub-system in the ISAC system can be expressed as [5], [13]

$$\mathbf{y}^e(t) = \mathbf{H}^e(t, f)\mathbf{s}(t) + \mathbf{n}^e(t), \tag{1}$$

where $\mathbf{n}^e(t) \in \mathbb{C}^{M_{R^e} \times 1}$ is the noise component, $\mathbf{H}^e(t, f) = \int \mathbf{H}^e(t, \tau) e^{-j2\pi f \tau} d\tau$ represents the frequency domain sensing

channel matrix with $\mathbf{H}^e(t, \tau) = \left[h_{pq^e}^e(t, \tau) \right]_{M_{R^e} \times M_T}$ denoting its time domain counterpart. In particular, $h_{pq^e}^e(t, \tau)$ is the complex channel impulse response (CIR) including path loss between the p-th ($p = 1, 2, ..., M_T$) BS transmit antenna and the q^e-th ($q^e = 1, 2, ..., M_{R^e}$) echo receiving antenna in the sensing sub-system, which is composed of three components

$$h_{pq^e}^e(t, \tau) = h_{pq^e}^{e,\text{MR}}(t, \tau) + h_{pq^e}^{e,\text{static}}(t, \tau) + h_{pq^e}^{e,\text{mobile}}(t, \tau), \tag{2}$$

where $h_{pq^e}^{e,\text{MR}}(t, \tau)$, $h_{pq^e}^{e,\text{static}}(t, \tau)$, and $h_{pq^e}^{e,\text{mobile}}(t, \tau)$ are the CIRs of the links corresponding to terminal target MR, static targets in set C_{L_1}, and mobile targets in set C_{L_2}, respectively. Here we have to mention that the CIR of the link for static target in set C_{L_1} is time-invariant, thus we can simplify $h_{pq^e}^{e,\text{static}}(t, \tau)$ into $h_{pq^e}^{e,\text{static}}(\tau)$. Furthermore, their expressions are presented as

$$
\begin{aligned}
h_{pq^e}^{e,\text{MR}}(t, \tau) = {} & \sqrt{\Omega_{\text{MR}}^e(t)} e^{-j \frac{2\pi}{\lambda} (\xi_{\text{MR}}^T(t) + \xi_{\text{MR}}^{R^e}(t))} \\
& \times e^{j \frac{2\pi}{\lambda} \langle e_T^{\text{MR}}(t), \mathbf{d}_p^T \rangle} e^{j \frac{2\pi}{\lambda} \langle e_{R^e}^{\text{MR}}(t), \mathbf{d}_{q^e}^{R^e} \rangle} \\
& \times e^{j \frac{2\pi}{\lambda} \langle -\mathbf{v}_R t, e_T^{\text{MR}}(t) \rangle} e^{j \frac{2\pi}{\lambda} \langle -\mathbf{v}_R t, e_{R^e}^{\text{MR}}(t) \rangle} \\
& \times \delta\left(\tau - \left(\xi_{\text{MR}}^T(t) + \xi_{\text{MR}}^{R^e}(t) \right) / c \right),
\end{aligned} \tag{3}
$$

$$
\begin{aligned}
h_{pq^e}^{e,\text{static}}(\tau) = {} & \sum_{\ell_1=1}^{L_1} \sqrt{\Omega_{s_{\ell_1}}^e} e^{-j \frac{2\pi}{\lambda} (\xi_{s_{\ell_1}}^T + \xi_{s_{\ell_1}}^{R^e})} \\
& \times e^{j \frac{2\pi}{\lambda} \langle e_T^{s_{\ell_1}}, \mathbf{d}_p^T \rangle} e^{j \frac{2\pi}{\lambda} \langle e_{R^e}^{s_{\ell_1}}, \mathbf{d}_{q^e}^{R^e} \rangle} \\
& \times \delta\left(\tau - (\xi_{s_{\ell_1}}^T + \xi_{s_{\ell_1}}^{R^e}) / c \right),
\end{aligned} \tag{4}
$$

$$
\begin{aligned}
h_{pq^e}^{e,\text{mobile}}(t, \tau) = {} & \sum_{\ell_2=1}^{L_2} \sqrt{\Omega_{s_{\ell_2}}^e(t)} e^{-j \frac{2\pi}{\lambda} (\xi_{s_{\ell_2}}^T(t) + \xi_{s_{\ell_2}}^{R^e}(t))} \\
& \times e^{j \frac{2\pi}{\lambda} \langle e_T^{s_{\ell_2}}(t), \mathbf{d}_p^T \rangle} e^{j \frac{2\pi}{\lambda} \langle e_{R^e}^{s_{\ell_2}}(t), \mathbf{d}_{q^e}^{R^e} \rangle} \\
& \times e^{j \frac{2\pi}{\lambda} \langle -\mathbf{v}_{\ell_2} t, e_T^{s_{\ell_2}}(t) \rangle} e^{j \frac{2\pi}{\lambda} \langle -\mathbf{v}_{\ell_2} t, e_{R^e}^{s_{\ell_2}}(t) \rangle} \\
& \times \delta\left(\tau - \left(\xi_{s_{\ell_2}}^T(t) + \xi_{s_{\ell_2}}^{R^e}(t) \right) / c \right),
\end{aligned} \tag{5}
$$

where $c = 3.0 \times 10^8$ m/s, $\Omega_{\text{MR}}^e(t) = \frac{\lambda^2 \sigma_{\text{MR}}}{(4\pi)^3 (\xi_{\text{MR}}^T(t) \xi_{\text{MR}}^{R^e}(t))^2}$, $\Omega_{s_{\ell_1}}^e = \frac{\lambda^2 \sigma_{s_{\ell_1}}}{(4\pi)^3 (\xi_{s_{\ell_1}}^T \xi_{s_{\ell_1}}^{R^e})^2}$, and $\Omega_{s_{\ell_2}}^e(t) = \frac{\lambda^2 \sigma_{s_{\ell_2}}}{(4\pi)^3 (\xi_{s_{\ell_2}}^T(t) \xi_{s_{\ell_2}}^{R^e}(t))^2}$ denote the path power gains including the path loss of the sensing links for target MR, static target s_{ℓ_1}, and mobile target s_{ℓ_2}, respectively. The σ_{MR}, $\sigma_{s_{\ell_1}}$, and $\sigma_{s_{\ell_2}}$ are the radar cross section (RCS) of the corresponding targets, whose typical values are given in Table II [13]. The $\mathbf{d}_p^T$ and $\mathbf{d}_{q^e}^{R^e}$ represent the distance vectors from the centers of the signal transmitting and echo receiving ULAs to the p-th transmit and q^e-th echo receive antennas, respectively, and they are expressed as

$$\mathbf{d}_{i_1}^{T/R^e} = \frac{M_{T/R^e} - 2i_1 + 1}{2} \delta_{T/R^e} \begin{bmatrix} \cos \phi_{T/R^e} \cos \psi_{T/R^e} \\ \cos \phi_{T/R^e} \sin \psi_{T/R^e} \\ \sin \phi_{T/R^e} \end{bmatrix}, \tag{6}$$

where $i_1 = p$ for transmit antenna, e.g., $\mathbf{d}_p^T$, and $i_1 = q^e$ for echo receive antenna, e.g., $\mathbf{d}_{q^e}^{R^e}$, respectively. In addition,

$\left\{\boldsymbol{e}^{\mathrm{MR}}_{T/R^e}(t), \boldsymbol{e}^{s_{\ell_1}}_{T/R^e}, \boldsymbol{e}^{s_{\ell_2}}_{T/R^e}(t)\right\}$ denote the unit directional vectors from transmitting/echo receiving ULA to target MR, static target s_{ℓ_1}, and mobile target s_{ℓ_2}, respectively, which contain the location information of the targets and can be expressed as

$$\boldsymbol{e}^{i_2}_{T/R^e}(t) = \begin{bmatrix} \cos\beta^{i_2}_{T/R^e}(t)\cos\alpha^{i_2}_{T/R^e}(t) \\ \cos\beta^{i_2}_{T/R^e}(t)\sin\alpha^{i_2}_{T/R^e}(t) \\ \sin\beta^{i_2}_{T/R^e}(t) \end{bmatrix}, \quad (7)$$

where $i_2 \in \{\mathrm{MR}, s_{\ell_1}, s_{\ell_2}\}$, and for static target s_{ℓ_1} we have $\alpha^{s_{\ell_1}}_{T/R^e}(t) = \alpha^{s_{\ell_1}}_{T/R^e}$ and $\beta^{s_{\ell_1}}_{T/R^e}(t) = \beta^{s_{\ell_1}}_{T/R^e}$, respectively.

It is worth mentioning that the CIRs in (2)-(5) is a general description of the channel response of the sensing sub-system in ISAC system, which can be adapted for characterizing both monostatic and bistatic sensing scenarios. Specifically, in monostatic sensing scenario, the echo links from sensing targets to echo receiving ULA share the same distance and angle parameters as the transmission links from transmitting ULA to the sensing targets, indicting that $\xi_{R^e,\mathrm{MR}}(t) = \xi_{T,\mathrm{MR}}(t)$, $\xi_{R^e,s_{\ell_1}} = \xi_{T,s_{\ell_1}}$, $\xi_{R^e,s_{\ell_2}}(t) = \xi_{T,s_{\ell_2}}(t)$, $\alpha^{\mathrm{MR}}_T(t) = \alpha^{\mathrm{MR}}_{R^e}(t)$, $\beta^{\mathrm{MR}}_T(t) = \beta^{\mathrm{MR}}_{R^e}(t)$, $\alpha^{s_{\ell_1}}_T = \alpha^{s_{\ell_1}}_{R^e}$, $\beta^{s_{\ell_1}}_T = \beta^{s_{\ell_1}}_{R^e}$, $\alpha^{s_{\ell_2}}_T(t) = \alpha^{s_{\ell_2}}_{R^e}(t)$, and $\beta^{s_{\ell_2}}_T(t) = \beta^{s_{\ell_2}}_{R^e}(t)$, respectively. Furthermore, by exploiting the matched-filtering or other advanced estimation technologies [5], it is reasonable to assume that the distance and angle parameters of the targets can be well sensed.

B. Communication Channel Modeling

In the communication channel, the transmitted signals from the BS will travel through LoS path, NLoS paths with static clusters, and NLoS paths with mobile clusters to the communication receiver MR. We assume there are L_3 static clusters forming a cluster set of C_{L_3}, in which the ℓ_3-th ($\ell_3 = 1, 2, ..., L_3$) cluster is denoted by s_{ℓ_3}, and assume there are L_4 mobile clusters forming a cluster set of C_{L_4} with the ℓ_4-th ($\ell_4 = 1, 2, ..., L_4$) cluster being denoted by s_{ℓ_4}, respectively. Each cluster contributes a multipath propagation link with I rays. The velocity vector of the mobile cluster s_{ℓ_4} is $\mathbf{v}_{\ell_4} = v_{\ell_4}[\cos\gamma_{\ell_4}, \sin\gamma_{\ell_4}, 0]^T$ with v_{ℓ_4} and γ_{ℓ_4} denoting the moving speed and direction, respectively. We denote $\mathbf{y}^c(t) \in \mathbb{C}^{M_R \times 1}$ as the MR received signal vector, $\mathbf{n}^c(t) \in \mathbb{C}^{M_R \times 1}$ as the noise vector, and $\mathbf{H}^c(t, f) = \int \mathbf{H}^c(t, \tau)e^{-j2\pi f\tau}d\tau$ as the frequency domain communication channel matrix, respectively. The received signal model for the communication sub-system in the ISAC system yields to be [10], [12]

$$\mathbf{y}^c(t) = \int \mathbf{H}^c(t, \tau)e^{-j2\pi f\tau}d\tau\, \mathbf{s}(t) + \mathbf{n}^c(t), \quad (8)$$

where $\mathbf{H}^c(t, \tau) = \left[h^c_{pq}(t, \tau)\right]_{M_R \times M_T}$ is the time domain communication channel matrix and $h^c_{pq}(t, \tau)$ denotes the CIR between the p-th BS transmit antenna and q-th ($q = 1, 2, ..., M_R$) MR receive antenna in the communication sub-system, i.e.,

$$h^c_{pq}(t, \tau) = \sqrt{\Omega^c_{\mathrm{LoS}}(t)}h^{c,\mathrm{LoS}}_{pq}(t)\delta\big(\tau - \tau_{\mathrm{LoS}}(t)\big)$$

$$+ \sum_{\ell_3=1}^{L_3} \sqrt{\Omega^c_{s_{\ell_3}}(t)}h^{c,s_{\ell_3}}_{pq}(t)\delta\big(\tau - \tau_{\ell_3}(t)\big)$$

$$+ \sum_{\ell_4=1}^{L_4} \sqrt{\Omega^c_{s_{\ell_4}}(t)}h^{c,s_{\ell_4}}_{pq}(t)\delta\big(\tau - \tau_{\ell_4}(t)\big), \quad (9)$$

where $\tau_{\mathrm{LoS}}(t) = \xi^T_{\mathrm{MR}}(t)/c$, $\tau_{\ell_3}(t) = \big(\xi^T_{\ell_3} + \xi^R_{\ell_3}(t)\big)/c$, and $\tau_{\ell_4}(t) = \big(\xi^T_{\ell_4}(t) + \xi^R_{\ell_4}(t)\big)/c$ denote the propagation delays of the LoS path, NLoS path via static cluster s_{ℓ_3}, and NLoS path via mobile cluster s_{ℓ_4}, respectively. The $\Omega^c_{\mathrm{LoS}}(t) = \frac{\lambda^2}{(4\pi)^2\xi^{T}_{\mathrm{MR}}{}^2(t)}$, $\Omega^c_{s_{\ell_3}}(t) = \frac{\lambda^2 P_{\ell_3}(t)}{(4\pi)^2(\xi^T_{\ell_3} + \xi^R_{\ell_3}(t))^2}$, and $\Omega^c_{s_{\ell_4}}(t) = \frac{\lambda^2 P_{\ell_4}(t)}{(4\pi)^2(\xi^T_{\ell_4}(t) + \xi^R_{\ell_4}(t))^2}$ represent the path power gains including path loss of the LoS path, NLoS path via static cluster s_{ℓ_3}, and NLoS path via mobile cluster s_{ℓ_4}, respectively, in which $P_{\ell_3}(t)$ and $P_{\ell_4}(t)$ denote the powers of clusters s_{ℓ_3} and s_{ℓ_4}, respectively [14], [15]. Furthermore, $h^{c,\mathrm{LoS}}_{pq}(t)$, $h^{c,s_{\ell_3}}_{pq}(t)$, and $h^{c,s_{\ell_4}}_{pq}(t)$ are the CIRs between the (p,q)-th transmit-receive antenna pair of the LoS path, NLoS path via static cluster s_{ℓ_3}, and NLoS path via mobile cluster s_{ℓ_4}, respectively, and they can be expressed as

$$h^{c,\mathrm{LoS}}_{pq}(t) = e^{-j\frac{2\pi}{\lambda}\xi^T_{\mathrm{MR}}(t)} \times e^{j\frac{2\pi}{\lambda}\langle\boldsymbol{e}^{\mathrm{MR}}_T(t), \mathbf{d}^T_p\rangle}$$

$$\times e^{j\frac{2\pi}{\lambda}\langle-\boldsymbol{e}^{\mathrm{MR}}_T(t), \mathbf{d}^R_q\rangle} \times e^{j\frac{2\pi}{\lambda}\langle\mathbf{v}_R t, -\boldsymbol{e}^{\mathrm{MR}}_T(t)\rangle}, \quad (10)$$

$$h^{c,s_{\ell_3}}_{pq}(t) = \sqrt{\frac{1}{I}}\sum_{i_3=1}^{I} e^{j\left(\varphi_{\ell_3,i_3} - \frac{2\pi}{\lambda}\left(\xi^T_{\ell_3,i_3} + \xi^R_{\ell_3,i_3}(t)\right)\right)}$$

$$\times e^{j\frac{2\pi}{\lambda}\langle\boldsymbol{e}^{\ell_3,i_3}_T, \mathbf{d}^T_p\rangle} \times e^{j\frac{2\pi}{\lambda}\langle\boldsymbol{e}^{\ell_3,i_3}_R(t), \mathbf{d}^R_q\rangle}$$

$$\times e^{j\frac{2\pi}{\lambda}\langle\mathbf{v}_R t, \boldsymbol{e}^{\ell_3,i_3}_R(t)\rangle}, \quad (11)$$

$$h^{c,s_{\ell_4}}_{pq}(t) = \sqrt{\frac{1}{I}}\sum_{i_4=1}^{I} e^{j\left(\varphi_{\ell_4,i_4} - \frac{2\pi}{\lambda}\left(\xi^T_{\ell_4,i_4}(t) + \xi^R_{\ell_4,i_4}(t)\right)\right)}$$

$$\times e^{j\frac{2\pi}{\lambda}\langle\boldsymbol{e}^{\ell_4,i_4}_T(t), \mathbf{d}^T_p\rangle} \times e^{j\frac{2\pi}{\lambda}\langle-\mathbf{v}_{\ell_4} t, \boldsymbol{e}^{\ell_4,i_4}_T(t)\rangle}$$

$$\times e^{j\frac{2\pi}{\lambda}\langle\boldsymbol{e}^{\ell_4,i_4}_R(t), \mathbf{d}^R_q\rangle} \times e^{j\frac{2\pi}{\lambda}\langle(\mathbf{v}_R - \mathbf{v}_{\ell_4})t, \boldsymbol{e}^{\ell_4,i_4}_R(t)\rangle}, (12)$$

where $\left\{\varphi_{\ell_3,i_3}\right\}^{\ell_3=1,...,L_3}_{i_3=1,...,I}$ and $\left\{\varphi_{\ell_4,i_4}\right\}^{\ell_4=1,...,L_4}_{i_4=1,...,I}$ are assumed to be independent and uniformly distributed random phases. $\mathbf{d}^R_q = \frac{M_R - 2q + 1}{2}\delta_R[\cos\phi_R\cos\psi_R, \cos\phi_R\sin\psi_R, \sin\phi_R]^T$. The $\boldsymbol{e}^{\ell_3,i_3}_T$ and $\boldsymbol{e}^{\ell_3,i_3}_R(t)$ denote the unit directional vectors from BS transmitting and MR receiving ULAs to the static cluster s_{ℓ_3} via the i_3-th ($i_3 = 1, ..., I$) ray, respectively; whereas $\boldsymbol{e}^{\ell_4,i_4}_T(t)$ and $\boldsymbol{e}^{\ell_4,i_4}_R(t)$ are the uni directional vectors from BS transmitting and MR receiving ULAs to the mobile cluster s_{ℓ_4} via the i_4-th ($i_4 = 1, ..., I$) ray, respectively. Their expressions can be obtained from $\boldsymbol{e}^{\mathrm{MR}}_T(t)$ in (7) by replacing $\{\alpha^{\mathrm{MR}}_T(t), \beta^{\mathrm{MR}}_T(t)\}$ with $\{\alpha^{\ell_3,i_3}_T, \beta^{\ell_3,i_3}_T\}$, $\{\alpha^{\ell_3,i_3}_R(t), \beta^{\ell_3,i_3}_R(t)\}$, $\{\alpha^{\ell_4,i_4}_T(t), \beta^{\ell_4,i_4}_T(t)\}$, and $\{\alpha^{\ell_4,i_4}_R(t), \beta^{\ell_4,i_4}_R(t)\}$, respectively, which are omitted here for brevity.

Since the communication receiver MR is sensed as a target in the sensing channel, the time-varying model parameters of the LoS path can be provided by the sensing channel. For the NLoS paths, including NLoS paths via static and mobile clusters, the time-varying model parameters are obtained according to the geometrical relationship among transmit ULA, clusters,

and receive ULA, based on the initial location information of the clusters as well as the motion parameters of the MR and/or clusters, in which the initial location information of the clusters are generally generated randomly [16], [17]. In this paper, however, we consider the sensing channel and communication channel share some common clusters, and therefore the initial location information of the shared clusters could be provided by the sensing channel. For arbitrary shared cluster s_{ℓ_5}, i.e., $s_{\ell_5} \in \{C_{L_1} \cap C_{L_3}\}$ for shared static clusters or $s_{\ell_5} \in \{C_{L_2} \cap C_{L_4}\}$ for shared mobile clusters, the communication channel and sensing channel share the same propagation from transmit ULA to the shared cluster s_{ℓ_5}, indicating that the location information of s_{ℓ_5} could be sensed. Then, based on the sensed location information of the shared cluster s_{ℓ_5}, the time-varying distance and angle parameters of the propagation link via the shared cluster s_{ℓ_5} could be updated following the same procedure in [14], [16], [18]. The detailed expressions are omitted here due to space limitation.

III. CHANNEL CHARACTERISTICS

A. Time-varying Spatial CCF

The time-varying spatial cross-correlation function (CCF) characterize the correlation properties of the channel between two different links in the space domain, which is widely used as a metric to measure the spatial diversity of multi-antenna channels and is defined as [18]

$$\rho_{(p,q),(p',q')}(t, \Delta p, \Delta q) = \frac{\mathbb{E}[h_{pq}^*(t)h_{p'q'}(t)]}{\sqrt{\mathbb{E}[|h_{pq}(t)|^2]\mathbb{E}[|h_{p'q'}(t)|^2]}}, \quad (13)$$

where $\Delta p = |p'-p|\delta_T/\lambda$ and $\Delta q = |q'(q^{e'})-q(q^e)|\delta_{R(R^e)}/\lambda$ represent the normalized transmit antenna spacing and normalized receive antenna spacing, respectively. By substituting $h_{pq^e}^e(t, \tau)$ from (2)-(5) and $h_{pq}^c(t, \tau)$ from (9)-(12) into (13), we can obtain the normalized spatial CCF of the sensing channel $\rho_{(p,q^e),(p',q^{e'})}^e(t, \Delta p, \Delta q^e)$ and that of the communication channel $\rho_{(p,q),(p',q')}^c(t, \Delta p, \Delta q)$, respectively. Their expressions are omitted here due to the space limitation.

B. Time-varying Temporal ACF

The time-varying temporal auto-correlation function (ACF) measures the correlation ratio of the link at two different time instants, where a smaller value of temporal ACF means a faster changing of the channel and hence requiring a more frequently estimation of the channel. The temporal ACF is defined as [18]

$$\rho_{(p,q)}(t, \Delta t) = \frac{\mathbb{E}[h_{pq}^*(t)h_{pq}(t + \Delta t)]}{\sqrt{\mathbb{E}[|h_{pq}(t)|^2]\mathbb{E}[|h_{pq}(t + \Delta t)|^2]}}, \quad (14)$$

where Δt is the time difference. The corresponding expression of the temporal ACF of the sensing channel and that of the communication channel can be obtained by substituting $h_{pq^e}^e(t, \tau)$ from (2)-(5) and $h_{pq}^c(t, \tau)$ from (9)-(12) into (14), respectively, whose expressions are omitted here for brevity.
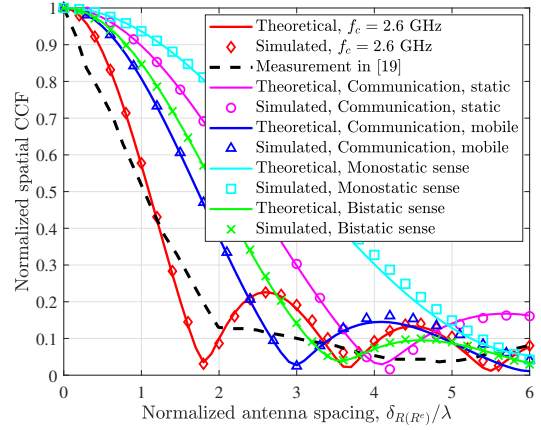

Fig. 2. Spatial CCF of the proposed ISAC channel model at $t = 2$ s, where 'Communication, static' means communication channel with static clusters.

IV. RESULTS AND DISCUSSIONS

In this section we numerically investigate the propagation characteristics of the proposed heterogeneous vehicular ISAC channel model. The ISAC system operates in the mmWave frequency band with $f_c = 28$ GHz, the parameter setting for the dual-function BS follows $H_0 = 30$ m, $M_T = 4$, $\delta_T = \lambda/2$, $\psi_T = \pi/3$, and $\phi_T = \pi/4$, respectively. For the communication sub-system, we set $\xi_R = 150$ m, $M_R = 6$, $\delta_R = \lambda/2$, $\psi_R = \pi/4$, and $\phi_R = \pi/4$, respectively. The communication receiver MR is in motion with speed $v_R = 5$ m/s and direction $\gamma_R = -\pi/6$, respectively. As the sensing sub-system is concerned, in monostatic sensing scenario the sensing echo receiver shares the same hardware as the dual-functional BS, thus having the same parameter setting. In bistatic sensing scenario, on the other hand, we set $x_{R^e} = 100$ m, $y_{R^e} = -30$ m, and $z_{R^e} = 30$ m, $M_{R^e} = 4$, $\delta_{R^e} = \lambda/2$, $\psi_{R^e} = \pi/3$, and $\phi_{R^e} = \pi/4$, respectively.

By exploiting (13), Fig. 2 compares the normalized spatial CCF of the proposed ISAC channel model in different components when $t = 2$ s, where the results show that the spatial correlations of both communication and sensing channels decrease gradually as the antenna spacing increases [9]. The results indicate that the communication and sensing channels show different spatial correlation properties even when the shared cluster is considered, which could be interpreted by the fact that the propagations from the shared cluster to the receivers in communication and sensing channels are independent. Moreover, Fig. 2 shows that the communication channel with mobile clusters show faster decline of the spatial CCF as compared to that with static clusters, which is mainly because that more dynamics involved in the channel will cause faster vary of the channel and thus helps improve the channel spatial diversity. In addition, it is seen from Fig. 2 that the bistatic sensing channel show smaller spatial correlation than monostatic sensing channel, thus is more benefit for channel spatial diversity. The larger spatial CCF of sensing channel confirms that it is more sparse than communication channel because of more concentrated signal propagation. It is also
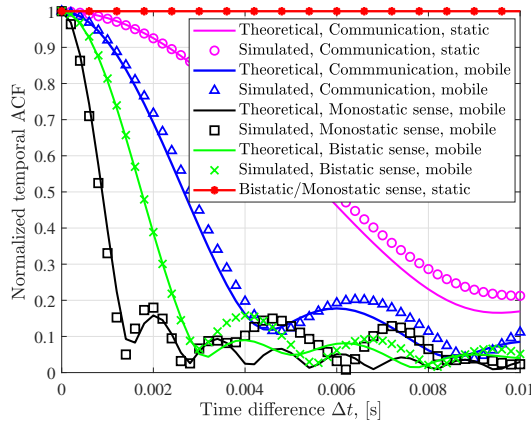
Fig. 3. Temporal ACF of the proposed ISAC channel model at $t = 5$ s, where 'Communication, static' means communication channel with static clusters.

seen from Fig. 2 that the simulated results match with the theoretical ones well, which confirms the correctness of the derived spatial CCF of the proposed ISAC channel model; meanwhile, the negligible difference between measurement results from [19] and theoretical/simulated ones under $f_c = 2.6$ GHz confirms the accuracy of the proposed channel model.

In Fig. 3, we study the temporal correlation properties of the proposed ISAC channel model for different propagation links at $t = 5$ s based on (14). The results show that the sensing channel with mobile targets/clusters show faster decline of the temporal ACF than communication channel, which means the sensing channel is more sensitive to the targets/clusters motion and changes more rapidly, arising for more frequent estimation of the channel. Also, it reveals that the monostatic sensing channel show smaller temporal correlation than bistatic sensing channel, requiring more transmission resources for channel estimation, which should be well balanced in resource-limited ISAC system design. As for the communication channel, it is seen from Fig. 3 that the channel with mobile clusters has smaller and faster decreasing of temporal ACF as it involves more dynamics, which is in agreement with our previous results in [16]. Finally, the excellent agreement between simulated and theoretical curves verify the effectiveness of the proposed ISAC channel model.

V. Conclusion

In this paper, we have considered the channel modeling of a multi-antenna heterogeneous vehicular ISAC system, where a dual-functional BS communicates with the MR and senses the surrounding environments simultaneously. By adopting the cluster-based structure, the channel responses of the sensing and communication channels considering the presence of both static as well as mobile targets/clusters are respectively derived, which are partially correlated with each other through the shared targets/clusters. The proposed ISAC channel model can be adapted for both monostatic and bistatic sensing scenarios. These make the proposed model superior to existing ones. The results reveal that the communication and sensing

channels show different propagation properties, and the sensing channel is more sensitive to mobile targets. The agreement between theoretical and simulated as well as measurement results validate the effectiveness of the proposed model.

As a promising enable technology in 6G network, the channel modeling research on ISAC still has a long way to go. Due to the space limitation, more detailed derivations of the proposed ISAC channel model, discussions on the propagation characteristics as well as the cross-correlations between communication and sensing channels, and performance analysis on the model are left in the extended version of this paper.

References

[1] W. Saad, M. Bennis, and M. Chen, "A vision of 6G wireless systems: Applications, trends, technologies, and open research problems," *IEEE Netw.*, vol. 34, no. 3, pp. 134-142, May/Jun. 2020.

[2] Y. Cui, F. Liu, X. Jing, and J. Mu, "Integrating sensing and communications for ubiquitous IoT: Applications, trends, and challenges," *IEEE Netw.*, vol. 35, no. 5, pp. 158-167, Sep. 2021.

[3] X. Shen, J. Li, L. Chen, J. Chen, and S. He, "Heterogeneous LTE/DSRC approach to support real-time vehicular communications," in *Proc. ICAIT*, Stockholm, Sweden, Aug. 2018, pp. 122-127.

[4] Q. Zhang *et al.*, "Design and performance evaluation of joint sensing and communication integrated system for 5G mmWave enabled CAVs,"*IEEE J. Sel. Topics Signal Process.*, vol. 15, no. 6, pp. 1500-1514, Nov. 2021.

[5] F. Liu *et al.*, "Radar-assisted predictive beamforming for vehicular links: Communication served by sensing," *IEEE Trans. Wireless Commun.*, vol. 19, no. 11, pp. 7704-7719, Nov. 2020.

[6] H. Jiang, B. Xiong, H. Zhang, and E. Basar, "Hybrid far- and near-field modeling for reconfigurable intelligent surface assisted V2V channels: A sub-array partition based approach," *IEEE Trans. Wireless Commun.*, early access, doi: 10.1109/TWC.2023.3262063.

[7] X. Li, J. He, Z. Yu, G. Wang, and P. Zhu, "Integrated sensing and communication in 6G: the deterministic channel models for THz imaging," in *Proc. IEEE PIMRC*, Helsinki, Finland, Sep. 2021, pp. 1-6.

[8] Z. Zhang, R. He, B. Ai, M. Yang, C. Li, H. Mi, and Z. Zhong, "A general channel model for integrated sensing and communication scenarios," *IEEE Commun. Mag.*, vol. 61, no. 5, pp. 68-74, May 2023.

[9] R. Yang *et al.*, "A novel 6G ISAC channel model combining forward and backward scattering," *IEEE Trans. Wireless Commun.*, early access, doi: 10.1109/TWC.2023.3258150.

[10] O. El Ayach, S. Rajagopal, S. Abu-Surra, Z. Pi, and R. W. Heath Jr., "Spatially spare precoding in millimeter wave MIMO systems," *IEEE Trans. Wireless Commun.*, vol. 13, no. 3, pp. 1499-1513, Mar. 2014.

[11] E. Fishler, A. Haimovich, R. Blum, D. Chizhik, L. Cimini, and R. Valenzuela, "MIMO radar: An idea whose time has come," in *Proc. IEEE Radar Conf.*, Philadelphia, PA, USA, Apr. 2004, pp. 71-78.

[12] B. Xiong, Z. Zhang, and H. Jiang, "Reconfigurable intelligent surface for mmWave mobile communications: What if LoS path exists?" *IEEE Wireless Commun. Lett.*, vol. 12, no. 2, pp. 247-251, Feb. 2023.

[13] C. A. Balanis, *Antenna Theory: Analysis and Design*. Hoboken, NJ, USA: Wiley, 2016.

[14] H. Jiang *et al.*, "Physics-based 3D end-to-end modeling for double-RIS assisted non-stationary UAV-to-ground communication channels," *IEEE Trans. Commun.*, vol. 71, no. 7, pp. 4247-4261, Jul. 2023.

[15] *Study on Channel Model for Frequencies From 0.5 to 100 GHz*, document 3GPP TR 38.901, Version 16.1.0, Release 16, Dec. 2019.

[16] B. Xiong, Z. Zhang, J. Zhang, *et al.*, "Novel multi-mobility V2X channel model in the presence of randomly moving clusters," *IEEE Trans. Wireless Commun.*, vol. 20, no. 5, pp. 3180-3195, May 2021.

[17] D. Xu *et al.*, "Robust and secure resource allocation for ISAC systems: a novel optimization framework for variable-length snapshots," *IEEE Trans. Wireless Commun.*, vol. 70, no. 12, pp. 8196-8214, Dec. 2022.

[18] B. Xiong, Z. Zhang, H. Jiang, J. Zhang, L. Wu, and J. Dang, "A 3D non-stationary MIMO channel model for reconfigurable intelligent surface auxiliary UAV-to-ground mmWave communications," *IEEE Trans. Wireless Commun.*, vol. 21, no. 7, pp. 5658-5672, Jul. 2022.

[19] S. Payami and F. Tufvesson, "Channel measurements and analysis for very large array system at 2.6 GHz," in *Proc. EUCAP*, Prague, Czech Republic, Mar. 2012, pp. 433-437.